RevMexAA (Serie de Conferencias), **30**, 72–79 (2007)

THE CASSIOPEIA A SUPERNOVA REMNANT IN X-RAYS

J. Martin Laming[1] and Una Hwang[2]

RESUMEN

Revisamos el progreso alcanzado hasta la fecha en el análisis del proyecto de observación "1 million second *Chandra* Very Large Project (VLP)" en el remanente de supernova Cassiopeia A. Exploramos la posibilidad de que Cas A explotase en un "burbuja". El viento de supergigante roja dentro del cual se expande la onda de choque de la explosión, fue posiblemente seguido por un período corto de viento tenue y rápido de Wolf-Rayet previo a la explosión, dejando una región de baja densidad en el centro, rodeado por el viento de supergigante roja de mayor densidad. También revisamos el estado actual de las observaciones de rayos X duros y la determinación de la masa de ^{44}Ti que se piensa que se eyectó en la explosión, con miras a las restricciones que esto pone a la explosión en si misma, y dónde se puedan encontrar los productos del decaimiento del ^{44}Ti.

ABSTRACT

We review progress to date on analysis of the 1 million second *Chandra* Very Large Project (VLP)observation of the Cassiopeia A supernova remnant. We explore the possibility that Cas A exploded into a "bubble". The red supergiant wind into which its blast wave is currently expanding, was possibly followed by a short period of fast tenuous Wolf-Rayet wind prior to explosion, leaving a low density region at the center, surrounded by higher density red supergiant wind. We also review the current state of hard X-ray observations and determination of the mass of ^{44}Ti thought to have been ejected in the explosion, with a view to the constraints this places on the nature of the explosion itself, and where in the remnant ^{44}Ti decay products are likely to be found.

Key Words: **SUPERNOVAE: INDIVIDUAL (CASSIOPEIA A) — SUPERNOVA REMNANTS**

1. INTRODUCTION

Core-collapse supernovae remain one of the most perplexing unsolved problems in modern astrophysics. Upon exhaustion of its nuclear fuel, the Fe core of a massive star increases in size, approaching the Chandrasekhar limit. Collapse of the core to nuclear density ensues, whereupon the stiffening of the equation of state halts the collapse and allows the core to "bounce". A shock wave is thus initiated and works its way outward, depositing energy into the outlying stellar layers and enabling further nucleosynthesis. The direct observables of such a collapse are gravitational waves, which remain to be detected from any source, and neutrinos, of which 20 electron antineutrinos were detected from SN 1987A (e.g., Bahcall 1989). While this represents a triumph of experimental physics, 20 electron antineutrinos remain just a detection, with little real diagnostic value. Fortunately, many details of the core-collapse mechanism are also imprinted in the Fe ejecta formed in the innermost layers of the star. The characteristics of the Fe are sensitive to the details of the explosion mechanism, including the mass and momentum imparted to the compact stellar remnant.

For decades, simulations of core-collapse supernovae had little success in producing explosions, with the emerging supernova shock stalling as it fought its way through the star. Recent multi-dimensional simulations of core-collapse supernovae, however, show how the development of instabilities can help to revive the stalled supernova shock front toward explosion (e.g. Burrows et al. 2006; Scheck et al. 2006; Kifonidis et al. 2005; Blondin & Mezzacappa 2006; Blondin et al. 2003). At the same time, observations have also improved dramatically. The most important advance here is the exquisite 0.5″ angular resolution provided in X-rays by the mirrors on the Chandra Observatory. This is exploited to the full by the 10^6 s 2004 observation of the Cassiopeia A SNR that allows us to identify individual compact ejecta fragments. The angular resolution of the *Chandra* mirrors has never before been attained in X-rays, nor will it be rivalled during our research lifetimes by any of the X-ray missions now being planned.

The ejecta in supernova remnants (SNRs) emit X-rays after passing through an inner (reverse) shock that starts at the interface (contact discontinuity)

[1]Naval Research Laboratory, Code 7674L, Washington DC 20375, USA (laming@nrl.navy.mil).

[2]NASA Goddard Space Flight Center, Code 662, Greenbelt MD 20771 and Department of Physics and Astronomy, Johns Hopkins University, 3400 Charles Street, Baltimore, MD 21218, USA (hwang@orfeo.gsfc.nasa.gov).

between the ejecta and the interstellar material swept up by the primary outer blast wave. The energetics make X-rays the characteristic emission of plasmas heated by the passage of these shocks. In young remnants, the reverse shocked ejecta often dominate the X-ray emission by virtue of their high densities and enriched composition, making the supernova ejecta accessible for study hundreds or thousands of years after the explosion.

The Galactic supernova remnant Cassiopeia A is an ideal candidate for such a study. It has a dynamical age of 330 yr (Thorstensen et al. 2001); young enough that the ejecta dominate the X-ray emission, and old enough that a substantial fraction of the ejecta have been heated by the reverse shock to X-ray emitting temperatures. It has been extremely well observed at all wavelengths, particularly in X-rays as the target of a recent 1 Ms observation with Chandra. Such a deep observation of a SNR is unprecedented in soft and medium energy X-rays. Given Cas A's intrinsic brightness, these data provide moderate resolution X-ray spectra at the $0.5''$ scale of the Chandra mirrors for nearly the entire $5'$ extent of the supernova remnant. Of equal importance, X-ray observations reveal the shocked inner ejecta layers in Cas A, including Si and Fe that were synthesized during the explosion, making it the most compelling target available for such studies.

2. HYDRODYNAMIC STATE

Cas A has long been known to have had a massive progenitor on the basis of optical emission dominated by O, since oxygen is synthesized hydrostatically by massive stars during their lifetimes. During their evolution massive stars undergo mass loss that generates a circumstellar wind environment (often idealized as a $\rho \propto r^{-2}$ density profile), before exploding as core-collapse supernovae (Type Ib/Ic with loss of H and/or He and variants of II). They generally leave a compact stellar remnant behind, either neutron star or black hole, while exhibiting a wide range of properties that reflects the diversity of their progenitors (e.g., Filippenko 2001).

Cas A's progenitor probably had a main sequence mass of 15-25 $M_\odot$ (at the lower end of Wolf Rayet masses; Massey et al. (2001) see arguments given by Laming & Hwang 2003, hereafter LH03; and Chevalier & Oishi 2003). This inference is supported by studies of the fast-moving optical knots (Fesen et al. 1988). The progenitor mass was reduced to about 3-4 $M_\odot$ at the time of explosion by extensive mass loss, mainly in the red supergiant (RSG) phase, possibly with the aid of a binary companion. There is

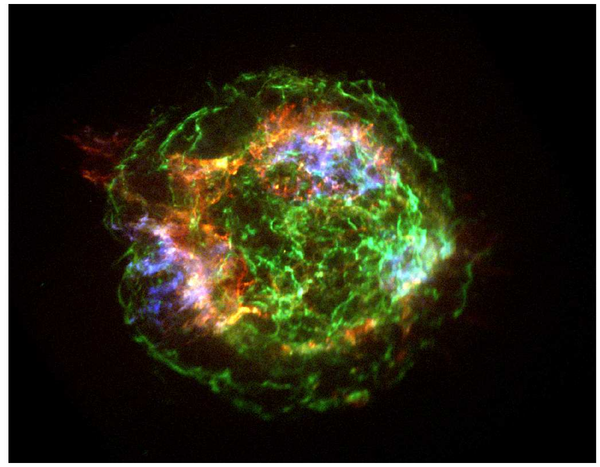

Fig. 1. Three-color 1 Ms Chandra ACIS image of Cas A with red=Si He α, blue=Fe K, green=4-6 keV continuum from the blast wave. The clumpiness of the Si ejecta is evident.

speculation that Cas A actually exploded in a circumstellar bubble, we discuss possible evidence for this below from our X-ray observations, but for the most part, the remnant's blast wave has been propagating through the remains of this slow, dense RSG wind. About $2M_\odot$ of Cas A's ejecta have now been shock heated to emit X-ray (and optical) emission. This hydrodynamical model (derived by LH03 based on Truelove & McKee 1999) also accounts for the forward shock velocity and radius (Delaney & Rudnick 2003), the separation between reverse and forward shocks (Gotthelf et al. 2001), the emission measure and mass of the shocked circumstellar plasma (Willingale et al. 2002), and the temperatures and ionization ages of the ejecta knots.

A binary progenitor scenario becomes compelling for Cas A when observational constraints are weighed in the context of three-dimensional explosion calculations and stellar models for both single and binary stars. Young et al. (2006) specifically consider as criteria the presence of optically emitting N-rich high velocity ejecta, the ejecta mass and the compact remnant mass (both near 2 $M_\odot$), and the abundances of ^{44}Ti and ^{56}Ni. They conclude that a 15-25 $M_\odot$ progenitor that loses its hydrogen envelope to a binary companion is the best match to these observational constraints.

The apparently high degree of mass-loss incurred by the Cas A progenitor helps to explain the unusual clumpiness of the X-ray emitting ejecta in Cas A, which are organized into compact knots and filaments (see Figure 1).

In the two-dimensional core-collapse explosion models of Kifonidis et al. (2000, 2004), metal clumps are seen to survive and propagate outwards more readily in Type Ib explosions, where the core-collapse is preceded by loss of the H layer, compared to Type II explosions, which proceed with the H layer at least partially intact. Mixing of the ejecta during the explosion occurs by Rayleigh-Taylor instabilities. In Type II explosions, the blast wave decelerates in the dense He layer and generates a reverse shock that shreds and mixes the clumps so that at time 20,000s after bounce, almost all the metals are completely mixed throughout the inner 3.4 $M_{\odot}$. By contrast, pre-supernova mass loss suppresses Rayleigh-Taylor turbulence in Ib events because the resulting supernova has a much weaker reverse shock. This reduces the effect of the mixing instabilities so that metal clumps may survive and propagate further out into the ejecta. Rotation would further enhance the distribution of the metals throughout the ejecta (Hungerford et al. 2003).

3. SHOCK PHYSICS AND MODELS

The small size of Cas A's ejecta knots and properties related to their stability following shock passage are used to advantage by LH03 and Hwang & Laming (2003). A cloud or knot is accelerated differently by a shock than the ambient plasma, because the shock decelerates (accelerates) upon entering a higher (lower) density medium and may generate Kelvin-Helmholtz instability at the interface. Inside the cloud, the shock splits into transmitted and reflected shocks each time it encounters the boundary with the ambient plasma, and generates Rayleigh-Taylor or Richtmeyer-Meshkov instabilities (Klein, McKee, & Colella 1994; Poludnenko, Frank, & Blackman 2002; Poludnenko et al. 2004; Wang & Chevalier 2001). These instabilities destroy the cloud or knot within a few shock crossing times. The shock crossing time is 15-30 years for a 500-1000 km s^{-1} reverse shock passing through knots that are $1''$ (5×10^{16} cm) across, and is similar to the observed lifetimes of optical knots in Cas A (Thorstensen et al. 2001).

The apparent survival of individual X-ray knots for $\gg$ 30 years places an upper limit on their density relative to the surrounding plasma of a factor of $\sim$3 (see Table 3 of Klein, McKee, & Colella 1994)[3]. Moreover, the X-ray knots are of similar temperature to their surroundings and in general, do not coincide spatially with the fast moving optical ejecta knots. Hence we believe that the X-ray knots underwent reverse shock passage, and perhaps interacted with secondary shocks, early in Cas A's evolution. They are now expanding with the rest of the remnant plasma and have a similar density. This inference is supported by the X-ray proper motions measured for the blast wave and ejecta (DeLaney & Rudnick 2003). The short shock crossing time and the constraints on the density contrast allow a knot spectrum to be fitted with a single ionization age n_et, which can be plotted along with the fitted temperature T_e and compared with the results of models. This method allows Lagrangian mass coordinates (i.e., location) within the ejecta to be assigned to particular features. The element abundances as a function of this mass coordinate can then be compared to theoretical calculations.

Modeling is essential in deriving element abundances from X-ray spectra because of the large density gradients found in supernova remnants, particularly those like Cas A that are expanding into their presupernova stellar winds. To this end we have built a simulation code BLASPHEMER[4] (Laming & Hwang 2003; Laming & Grun 2002) which follows a Lagrangian plasma element through either the forward or reverse shock, integrating equations for the ionization balance, and electron and ion temperatures within a framework of analytic hydrodynamics based on self similar solutions for the SNR evolution. Ions and electrons undergo temperature jumps at shock proportional to their masses, followed by Coulomb equilibration. Collisionless equilibration appears to be more effective at lower velocity, or more properly, lower Alfvén Mach number shocks (Laming et al. 1996; Laming 1998, 2001a,b; Ghavamian et al. 2001, 2002; Rakowski, Ghavamian, & Hughes 2003; Ghavamian, Laming, & Rakowski 2006).

To explore the evolution of ejecta knots in a small bubble surrounded by circumstellar wind, we sampled Chandra spectra for radial series of knots in various locations of Cas A (shown in Figure 2), and fit models to determine the temperature and ionization age of the X-ray emitting gas. Typically, we find that two spectral components are needed to describe the spectra (with a separate component required for the Fe emission). For this purpose, however, we focus on the emission from ejecta other than Fe. Models were computed for ejecta with uniform density core and outer density profile power-law slopes n=9.7 (from Matzner & McKee 1999) evolving into bubble radii of 0, 0.2, and 0.3 pc within an other-

[3] These authors do not consider underdense knots, but the simulations of Blondin, Borkowski, & Reynolds (2001) suggest that these would be no less unstable.

[4] BLASt Propagation in Highly EMitting EnviRonment.

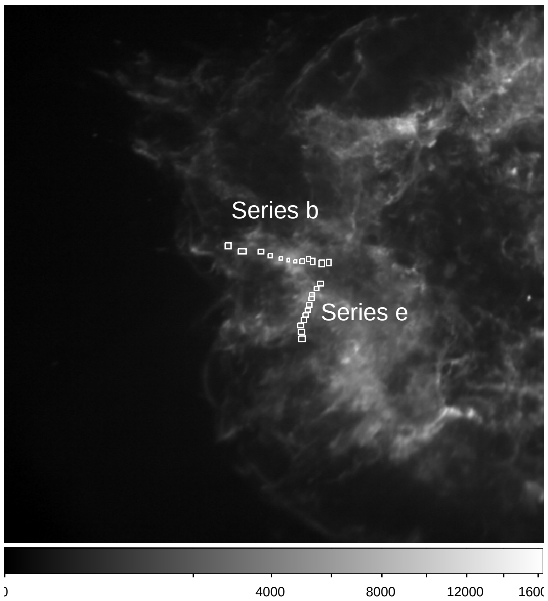

Fig. 2. Locations of knot series ("b" and "e") on the east limb of Cas A.

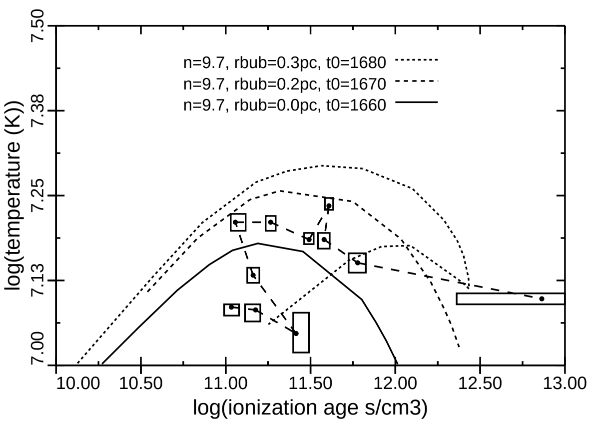

Fig. 3. Locus of temperature against ionization age for series b. Models with ejecta envelope power law of 9.7 for various bubble radii, compared with data points determined from single ionization age fits to knot spectra.

wise $1/r^2$ circumstellar wind, based in part on analytic results by Chevalier & Liang (1989). However these models have no swept up mass shell and the bubble boundary, they just transition directly to a $1/r^2$ wind density profile. Hence the implied explosion dates, which match the currently observed blast wave velocity and radius, are 1660, 1670, and 1680 AD, respectively. Recalling that the earliest possible explosion date is 1671 ± 1 (Thorstensen, Fesen, & van den Bergh 2001), a pure $1/r^2$ circumstellar medium

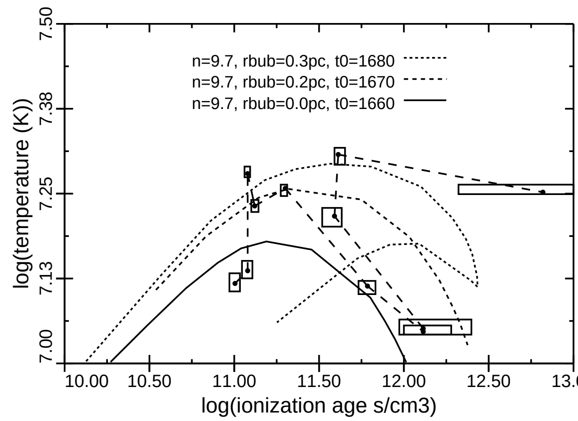

Fig. 4. Same as Figure 3 for series e.

would appear to be ruled out. More recent studies (Fesen et al. 2006b), accounting for possible deceleration of some of the optical knots, move the explosion date even later, albeit with larger uncertainties. The locus of temperature and ionization age evolution for each of the models is plotted in Figure 3 along with the values determined from spectral fits to the data. The size of the box for each data point indicates the 90% confidence error for the measured values.

In evaluating the figures, projection effects must be kept in mind. The fact that the Fe and Si ejecta require separate spectral components indicates the projection of these two different ejecta plasmas along the same relatively narrow (arcsecond angular scale) lines of sight. In addition, plasmas of similar composition but different temperature and ionization age may also be projected in the same manner. In general, such complications are expected to be worse in the interior regions of the remnant, for which the lines of sight through the remnant are longer. For example, in Figures 3 and 4, the first four regions of series b on the east limb are in the interior, and are expected to have the lowest ionization age. However, they do not fit well with the trend of increasing ionization age seen for the other knots, and are likely to suffer problems from projection. The remaining knots in the series are in fairly good agreement with a small bubble of 0.2 pc or slightly smaller. In series e (which crosses a line of optical filaments), the first two regions are also likely to be outliers caused by projection; projection may also play a role in the excursions for regions 6-8. The remaining regions are otherwise in resonably good agreement with the trend in ionization age and a bubble radius of $\sim$0.2 pc. Compared to the models without a bubble (as were presented in Laming &

Hwang 2003, and Hwang & Laming 2003), the inclusion of a small bubble tends to require a narrow range of steeper power laws (n=10,11 compared to n=6,7 and n=9,10), reducing the inferred degree of asymmetry in the remnant. The bubble models also allow for X-ray emitting knots with very high ionization age, at least some of which are indeed observed. The 0.2 pc model also gives the explosion date of 1671 AD that is determined from the dynamics of the optically emitting ejecta.

The one- and two-dimensional calculations of Dwarkadas (2005, 2006) for the evolution of a supernova blast wave into a calculated wind medium for a 35 $M_{\odot}$ progenitor show how different the evolution of a remnant in a wind-blown cavity can be from the evolution in either a constant density or uniform wind medium, with the structure, dynamics, and evolution all being affected. A very complex circumstellar bubble structure is established around massive stars by the interactions between the time-dependent winds during the star's evolution through the the main-sequence, red supergiant and Wolf-Rayet phases. To interpret the spectroscopic results, we do not need this full complexity, but our analytic models based so far on Chevalier & Liang (1989) remain to be fully validated against the analytic and numerical work in these and other references.

4. FE EJECTA AND ^{44}TI

The explosion that produced Cas A left its imprint on the composition of the supernova ejecta. Of the well-studied core-collapse remnants, Cas A most clearly reveals the inner ejecta layers of Si and Fe that were synthesized during the explosion. These elements have large-scale differences in their distribution, with the Fe rich products of complete Si burning being *exterior* to the lower Z elements in the southeast (Hughes et al. 2000; Hwang, Holt, & Petre 2002; see Figure 1). This indicates that some convective overturn has occurred between the ejecta layers. X-ray Doppler measurements of Si and Fe with *XMM-Newton*[5] (Willingale et al. 2002) show that the Si and Fe emission in the northwest are kinematically distinct, even though they overlap on the sky, with the Fe having a higher redshift and therefore being located behind (i.e., exterior to) the Si in that direction. Similar overturns are observed between the deeper S-, and overlying N-rich, optically emitting ejecta in the jet regions (Fesen 2001), but the overturns do not occur throughout the remnant since O- and N-rich optical knots are found external to the X-ray emitting Fe outside the jet (Fesen et al. 2006).

[5]at lower angular resolution than with *Chandra*

In explosively synthesizing Fe, Cas A underwent α-rich freezeout, wherein Si burns at the highest temperatures and low densities. The α-rich freezeout ashes are essentially pure ^{56}Ni (decaying to ^{56}Fe) along with residual He and trace amounts of certain elements such as radioactive ^{44}Ti, which decays via ^{44}Sc to ^{44}Ca (e.g., Arnett 1996; Thielemann et al. 1996; The et al. 1998). Cas A is also the only source for which both decay products of ^{44}Ti have been clearly detected in gamma-rays and hard X-rays, giving an inferred ^{44}Ti mass of $1.8 \times 10^{-4} M_{\odot}$ (Iyudin et al. 1994; Iyudin et al. 1997; Vink et al. 2001; Vink & Laming 2003; Rothschild & Lingenfelter 2003). More recently, Renaud et al. (2006) revise this to $1.6^{+0.6}_{-0.3} \times 10^{-4} M_{\odot}$, from an analysis of *INTEGRAL/IBIS/ISGRI* data. Early *Chandra* observations reveal a faint knot in Cas A that is evidently made of nearly pure Fe, and is thus a possible product of α-rich freezeout(see Figures 3 and 4 in Hwang & Laming 2003). The position of this Fe in the ejecta (its mass coordinate) can be inferred from its ionization age and is similar to those for the other Fe knots. The Chandra VLP spectrum of the knot confirms its pure Fe composition (see Figure 5).

The distribution of the Fe ejecta also gives clues to the mixing processes that occur during supernovae. An initial quantitative measure of the mixing is given by the analysis of the Fe knot spectra in early Chandra data (Hwang & Laming 2003). The mass coordinates inferred (albeit with large uncertainties for the time being) are consistent with mixing of the Fe (and therefore ^{44}Ti) from the α-rich freezeout zone out to the O/Si interface, assuming a 25 $M_{\odot}$ progenitor. This extent of mixing is consistent with the formation of X-type SiC (silicon carbide) grains which have elevated ^{44}Ca abundances from ^{44}Ti formed during α-rich freezeout (e.g., Clayton et al. 2002).

The Fe knots studied by Hwang & Laming (2003) are notably absent above a maximum ionization age of about 10^{12} cm^{-3} s (see Figure 6). In our models, Fe knots that were shocked sufficiently early on at high densities (and consequently have high ionization ages) undergo radiative instability so that they will not be detectable in X-rays. The nondetection of Fe knots in X-rays with high ionization ages at large radii therefore does not necessarily indicate that they do not exist. Indeed, the transport of Ti (i.e., α-rich freezeout ash) to far outlying ejecta layers is implied by the existence of presolar graphite grains with embedded TiC and metal subgrains. To form

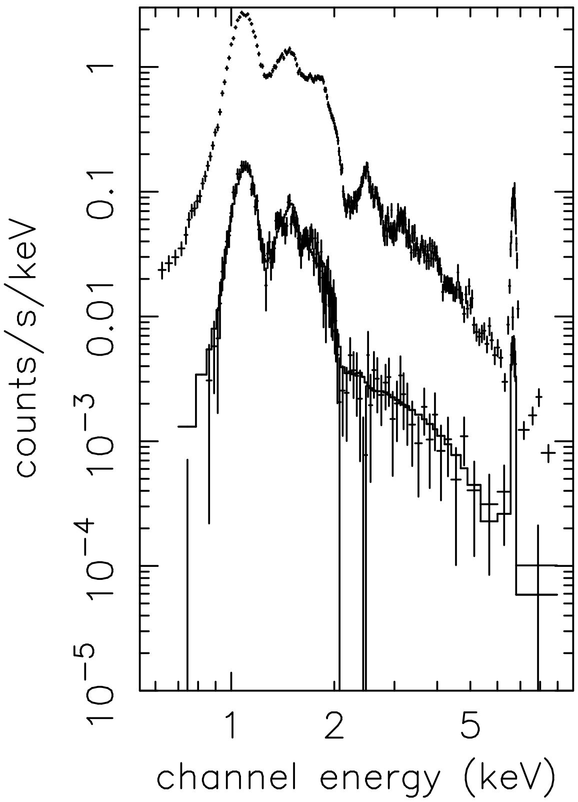

Fig. 5. Chandra spectra of a nearly pure Fe knot from 1 Ms observations (top; scaled by a factor of 10) and earlier observations (bottom).

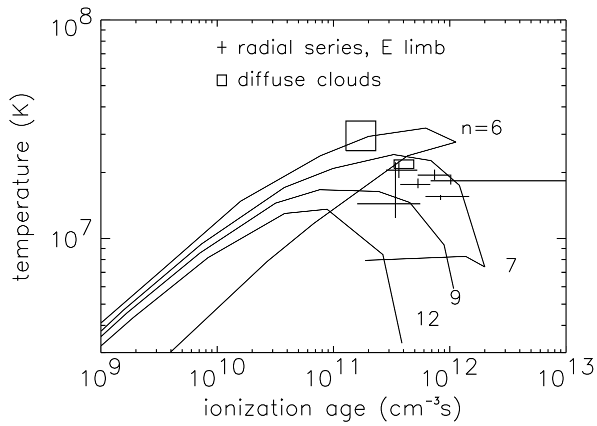

Fig. 6. Locus of temperature and ionization age for Fe-rich knots from Hwang & Laming (2003). The lower branch for each model with outer envelope power law n corresponds to reverse shock propagation through this envelope, the upper branch to reverse shock propagation through the uniform density ejecta core. The place where these meet at highest $n_e t$ is the ejecta core-envelope boundary. For $n > 7$, this region is radiatively unstable. Note the absence of knots with high ionization ages above $\sim 10^{12}$ cm^{-3}s, consistent with the thermal instability of knots shocked at early times in the models.

these grains, the Ti must be transported all the way to the graphite layers without undergoing substantial mixing with other nucleosynthesis layers, a feat that Lodders (2006) suggests might be accomplished by jets. There is little Fe detected in Cas A that is associated with the "jets", but some of the α-rich freezeout products were presumably transported to the outer graphite layers in the jet if these SN type graphite grains were formed. There they would then have already undergone radiative instability to temperatures below the X-ray regime, and might still be detectable through the innershell transition lines of the daughter products of ^{44}Ti, namely ^{44}Sc and ^{44}Ca.

Aside from the compositional evidence given by Lodders (2006), initial estimates of the ^{44}Ti mass in Cas A were sufficiently high that they led by themselves to suggestions that an asymmetric explosion involving jets might be required to sufficiently enhance the efficiency of α-rich freezeout (Nagataki et al. 1998). An alternative explanation, first put forward by Mochizuki et al. (1999), was that ^{44}Ti is sufficiently highly ionized behind the SNR reverse shock that the initial decay to ^{44}Sc by orbital electron capture is suppressed, which under the right conditions can lead to a higher than expected ^{44}Ti decay signal today. In Figure 7 we show the decay rate of ^{44}Ti in its various charge states from neutral (0+) to fully stripped (22+). The rates for ions are calculated using the FAC atomic code (Gu 2005) and scaled from the measurement for the neutral charge state (Görres et al. 1998; Ahmad et al. 1998). Every time an s electron is removed from the ion, the decay rate is reduced, since only s orbitals have non-zero probability density at the nucleus, but significant reductions in the decay rate only occur beyond the He-like charge state when 1s electrons are being ionized.

In Figures 8 and 9 we show sample evolutions of the ^{44}Ti ionization balance in an equatorial region of Cas A (parameters taken from Laming & Hwang 2003) and in the jet (parameters taken from Laming et al. 2006). In the equatorial region, an insignificant fraction of ^{44}Ti is ionized beyond the He-like charge state, and we conclude that rather low ($\sim 10\%$) changes to the ^{44}Ti decay rate will result. In the NE jet, the reverse shock is much stronger and the ^{44}Ti ionization balance is dominated by fully stripped and H-like charge states for about 100 years following reverse shock passage. Consequently in the

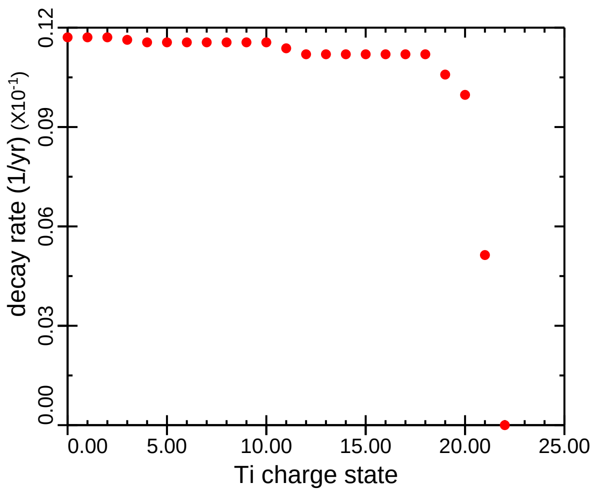

Fig. 7. Decay rate of ^{44}Ti in its various charge states. The decay rate is reduced every time an s electron is removed.

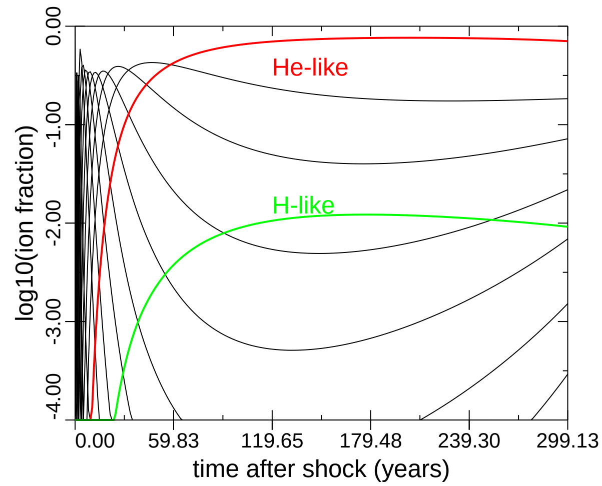

Fig. 8. Example . He-like is the dominant charge state, with only about 1% in the H-like charge state.

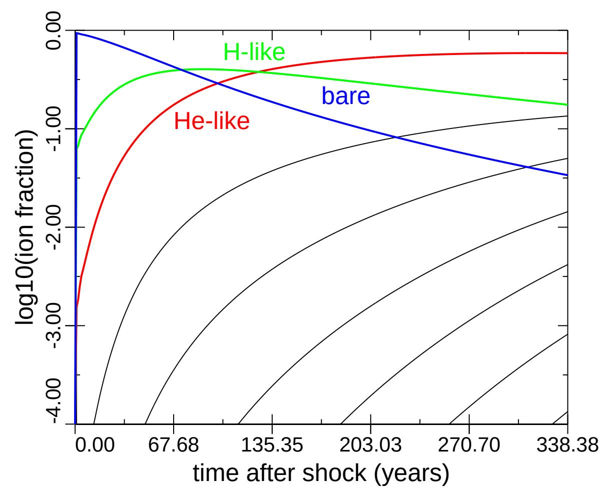

Fig. 9. Example ionization state of ^{44}Ti in the NE jet of Cas A as a function of time after reverse shock passage. Fully stripped and H-like charge state dominate for nearly 100 years following reverse shock passage.

jet region, substantial variations in the ^{44}Ti decay rate may result.

However, as mentioned above, significant quantities of Fe ejecta that should accompany the ^{44}Ti have not been detected in the NE jet. It is possible that cold Fe ejecta, invisible both in X-rays and in optical emission, are expanding at the head of the X-ray jet. Indeed, the jet models of Laming et al. (2006) require the existence of a substantial amount of radiatively cooled ejecta here. However attempts by these authors to find the inner shell K X-ray emission from ^{44}Sc and ^{44}Ca that also be emitted following the decay of ^{44}Ti have been unsuccesful so far. It is even possible that such emission lies at the extreme edge of, or even outside the *Chandra* field of view.

5. CONCLUSIONS

It is our belief that the 1 million second *Chandra* observation of the Cassiopeia A SNR, together with various supporting observations in other wavebands, represent a significant new body of data with which to explore the physics of core-collapse explosions in ways currently inaccessible to neutrino and gravitational wave observations. While Cas A might not be the result of a "normal" core-collapse event (if such a thing exists), the main reason for it being considered unusual, i.e. the high degree of presupernova mass loss, gives significant advantages in our analysis. The reverse shock has penetrated much further into the inner ejecta than would otherwise be the case, and we can hope to see in these ejecta traces of processes at work during the explosion itself. The other important feature of the mass loss is that sufficient clumps of inner ejecta survive to be observed in the remnant today, rather than being mixed with other ejecta by reverse shocks during the explosion. These clumps, and the spectrum fitting procedures enabled by their properties give us a distinct advantage in Cas A compared to other SNRs, where one generally has an uncertain line of sight integral over plasma shocked under different conditions. Even so, we expect a complete characterization of the ejecta emission to take several years of spectrum extraction, fitting and modeling.

This work was supported by the *Chandra* GO Program, the NASA LTSA Program, and by basic research funds of the Office of Naval Research.

REFERENCES

Ahmad, I., Bonino, G., Cini Castagnoli, G., Fischer, S. M., Kutschera, W., & Paul, M. 1998, Phys. Rev. Lett., 80, 2550

Arnett, D. 1996, Supernovae and Nucleosynthesis (Princeton: Princeton University Press)

Bahcall, J. N. 1989, Neutrino Astrophysics (Cambridge: Cambridge University Press)

Blondin, J. M., Borkowski, K. J., & Reynolds, S. P. 2001, ApJ, 557, 782

Blondin, J. M., & Mezzacappa, A. 2006, ApJ, 642, 401

Blondin, J. M., Mezzacappa, A., & DeMarino, C. 2003, ApJ, 584, 971

Burrows, A., Livne, E., Dessart, L., Ott, D. C., & Murphy, J. 2006, ApJ, 640, 878

Chevalier, R. A., & Liang, E. P. 1989,ApJ, 344, 332

Chevalier, R. A., & Oishi, J. 2003, ApJ, 593, L23

Clayton, D. D., Meyer, B. S., The, L.-S., & El-Eid, M. F. 2002, ApJ, 578, L83

DeLaney, T. A., & Rudnick, L. 2003, ApJ, 589, 818

Dwarkadas, V. V. 2005, ApJ, 630, 892

———. 2006, Ap&SS, 307, 153

Fesen, R. A. 2001, ApJS, 133, 161

Fesen, R. A., Becker, R. H., & Goodrich, R. W. 1988, ApJ, 329, L89

Fesen, R. A., et al. 2006a, ApJ, 636, 859

———. 2006b, ApJ, 645, 283

Filippenko, A. V. 2001, in AIP Conf. Proc. 565, Young Supernova Remnants, ed. S. S. Holt & U. Hwang (Melville: AIP), 40

Ghavamian, P., Laming, J. M., & Rakowski, C. E. 2006, ApJ, 654, L69

Ghavamian, P., Raymond, J. C., Smith, R. C., & Hartigan, P. 2001, ApJ, 547, 995

Ghavamian, P., Winkler, P. F., Raymond, J. C., & Long, K. S. 2002, ApJ, 572, 888

Görres, J., et al. 1998, Phys. Rev. Lett., 80, 2554

Gotthelf, E. V., Koralesky, B., Rudnick, L., Jones, T. W., Hwang, U., & Petre, R. 2001, ApJ, 552, L39

Gu, M. F. 2005, AIP Conf. Proc. 774, 'X-Ray Diagnostics of Astrophysical Plasmas: Theory, Experiment, and Observation, ed. R. K. Smith (Melville: AIP), 145

Hughes, J. P., Rakowski, C. E., Burrows, D. N., & Slane, P. O. 2000, ApJ, 528, L109

Hungerford, A. L., Fryer, C. L., & Warren, M. S. 2003, ApJ, 594, 390

Hwang, U., Holt, S. S., & Petre, R. 2000 ApJ, 537, L119

Hwang, U., & Laming, J. M. 2003, ApJ, 597, 362

Iyudin, A. F., et al. 1994, A&A, 284, L1

Iyudin, A. F., et al. 1997, in The Transparent Universe, ed. C. Winkler, T. J.-L. Courvoisier, & P. Durouchox (ESA SP-382; Noordwijk: ESA), 37

Kifonidis, K., Plewa, T., Janka, H.-T., & Müller, E. 2000, ApJ, 531, L123

———. 2004, A&A, 408, 624

Kifonidis, K., Plewa, T., Scheck, L., Janka, H.-T., & Müller, E. 2006, A&A, 453, 661

Klein, R. I., McKee, C. F., & Colella, P. 1994, ApJ, 420, 213

Laming, J. M. 1998, ApJ, 499, 309

Laming, J. M. 2001a, ApJ, 546, 1149

Laming, J. M. 2001b, ApJ, 563, 828

Laming, J. M., & Grun, J. 2002, Phys. Rev. Lett., 89, 125002

Laming, J. M., & Hwang, U. 2003, ApJ, 597, 347

Laming, J. M., Hwang, U., Radics, B., Lekli, G., & Takács, E. 2006, ApJ, 644, 260

Laming, J. M., Raymond, J. C., McLaughlin, B. M., & Blair, W. P. 1996, ApJ, 472, 267

Lodders, K. 2006, ApJ, 647, L37

Massey, P., DeGioia-Eastwood, K., & Waterhouse, E. 2001, AJ, 121, 1050

Matzner, C. D., & McKee, C. F. 1999, ApJ, 510, 379

Mochizuki, Y., Takahashi, K., Janka, H.-T., Hillebrandt, W., & Diehl R. 1999, A&A, 346, 831

Nagataki, S., Hashimoto, M., Sato, K., Yamada, S., & Mochizuki, Y. 1998, ApJ, 492, L45

Poludnenko, A. Y., Dannenberg, K. K., Drake, R. P., Frank, A., Knauer, J., Meyerhofer, D. D., Furnish, M., & Asay, J. R. 2004, ApJ, 604, 213

Poludnenko, A. Y., Frank, A., & Blackman, E. G. 2002, ApJ, 576, 832

Rakowski, C. E., Ghavamian, P., & Hughes, J. P. 2003, ApJ, 590, 846

Renaud, M., et al. 2006, ApJ, 647, L41

Rothschild, R. E., & Lingenfelter, R. E. 2003, ApJ, 582, 257

Scheck, L., Plewa, T., Janka, H.-Th., Kifonidis, K., & Müller, E. 2006, A&A, 457, 963

The, L.-S., Clayton, D. D., Jin, L., & Meyer, B. S. 1998, ApJ, 504, 500

Thielemann, F.-K., Nomoto, K., & Hashimoto, M. 1996, ApJ, 460, 408

Thorstensen, J. R., Fesen, R. A., & van den Bergh, S. 2001, AJ, 122, 297

Truelove, J. K., & McKee, C. F. 1999, ApJS, 120, 299; erratum ApJS, 128, 403

Vink, J., Laming, J. M., Kaastra, J. S., Bleeker, J. A. M., Bloemen, H., & Oberlack, U. 2001, ApJ, 560, L79

Vink, J., & Laming, J. M. 2003, ApJ, 584, 758

Wang, C.-Y., & Chevalier, R. A. 2001, ApJ, 549, 1119

Willingale, R., Bleeker, J. A. M., van der Heyden, K. J., Kaastra, J. S., & Vink, J. 2002, A&A, 381, 1039

Young, P. A., et al. 2006, ApJ, 640, 891